3D interferometric optical tweezers using a single spatial light modulator

Article *in* Optics Express · June 2005

DOI: 10.1364/OPEX.13.003777 · Source: PubMed

7 authors, including:

Johannes Courtial
University of Glasgow
188 PUBLICATIONS **10,591** CITATIONS

SEE PROFILE

Miles John Padgett
University of Glasgow
742 PUBLICATIONS **46,848** CITATIONS

SEE PROFILE

3D interferometric optical tweezers using a single spatial light modulator

Ethan Schonbrun, Rafael Piestun

Department of Electrical and Computer Engineering, University of Colorado, Boulder, Colorado, 80309
ethan.schonbrun@colorado.edu

Pamela Jordan, Jon Cooper

Department of Electrical and Electronic Engineering, University of Glasgow, Glasgow, G12 8QQ, UK

Kurt D Wulff

Department of Mechanical Engineering and Materials Science, Duke University, Durham, North Carolina, 27708

Johannes Courtial, Miles Padgett

Department of Physics and Astronomy, University of Glasgow, Glasgow, G12 8QQ, UK

Abstract: Hexagonal arrays of micron sized silica beads have been trapped in three-dimensions within an optical lattice formed by the interference of multiple plane-waves. The optical lattice design with sharply peaked intensity gradients produces a stronger trapping force than the traditionally sinusoidal intensity distributions of other interferometric systems. The plane waves were generated using a single, phase-only, spatial light modulator (SLM), sited near a Talbot image plane of the traps. Compared to conventional optical tweezers, where the traps are formed in the Fourier-plane of the SLM, this approach may offer an advantage in the creation of large periodic array structures. This method of pattern formation may also be applicable to trapping arrays of atoms.

OCIS Codes: (020.7010) Trapping, (170.4520) Optical confinement and manipulation, (090.1760) Computer holography, (090.2880) Holographic interferometry; (260.3160) Interference, (230.6120) Spatial light modulators.

References and Links

1. A. Ashkin, J. M. Dziedzic, J. E. Bjorkman and S. Chu, "Observation of a single-beam gradient force optical trap for dielectric particles," Opt. Lett. **11**, 288-290 (1986).
2. M. M. Burns, J. M. Fournier, and J.A. Golovchenko, "Optical matter: crystallization and binding in intense optical fields," Science, **249**, 749-754 (1990).
3. A. E. Chiou, W. Wang., G.J. Sonek, J. Hong, and M. W. Berns, "Interferometric optical tweezers," Optics Commun., **133**, 7-10 (1997).
4. P. Zemanek, A. Jonas, P. Jakl, J. Jezek, M. Sery, and M. Liska, "Theoretical comparison of optical traps created by standing wave and single beam," Opt Commun **220,** 401-412 (2003).
5. M. E. J. Friese, J. Enger, H. Rubinsztein-Dunlop and N. R. Heckenberg, "Optical angular-momentum transfer to trapped absorbing particles," Phys Rev A, **54**, 1593-1596 (1996).
6. H. He, N. R. Heckenberg and H. Rubinsztein-Dunlop, "Optical particle trapping with higher-order doughnut beams using high efficiency computer generated holograms," J. Mod. Opt, **42**(1), 217-223 (1995).
7. N. B. Simpson, L. Allen and M. J. Padgett, " Optical tweezers and optical spanners with Laguerre-Gaussian modes," J Mod Opt, **43**, 2485-2491 (1996).
8. D. G. Grier, "A revolution in optical manipulation," Nature, **424**, 810-816 (2003).
9. K. C. Neuman, S. M. Block, "Optical trapping" Review of Scientific Instruments, **75**, 2787-2809 (2004).
10. M. Reicherter, T. Haist, E. U. Wagemann and H. J. Tiziani, "Optical particle trapping with computer generated holograms written on a liquid crystal display," Opt. Lett. **24**, 608-610 (1999).
11. J. E. Curtis, B. A. Koss and D. G. Grier, "Dynamic holographic optical tweezers," Opt. Commun. **207**, 169-175 (2002).

#6962 - $15.00 US
Received 24 March 2005; revised 4 May 2005; accepted 5 May 2005

12. E. R. Dufresne, G. C. Spalding, M. T. Dearing, S. A. Sheets, D. G. Grier, "Computer-generated holographic optical tweezer arrays," Rev. Sci. Inst. **72,** 1810-1816 (2001).
13 G. Sinclair, P. Jordan, J. Leach, M. J. Padgett and J. Cooper, "Defining the trapping limits of holographic optical tweezers," J. Mod. Opt. **51**, 409-414 (2004).
14. G. Sinclair, P. Jordan, J. Courtial, M. Padgett, J. Cooper and Z. J. Laczik, "Assembly of 3-dimensional structures using programmable holographic optical tweezers," Opt. Express **12**, 5475 (2004). http://www.opticsexpress.org/abstract.cfm?URI=OPEX-12-22-5475.
15. R. Piestun and J. Shamir, "Control of wave-front propagation with diffractive elements," Opt. Lett. **19**, 771-773 (1994).
16. R. L. Eriksen, V. R. Daria, and J. Gluckstad, "Fully dynamic multiple-beam optical tweezers," Opt. Express **10**, 597-602 (2002). http://www.opticsexpress.org/abstract.cfm?URI=OPEX-10-14-597.
17. P.J. Rodrigo,V.R. Daria, J. Gluckstad, "Real-time three-dimensional optical micromanipulation of multiple particles and living cells," Opt Lett **29**, 2270-2272 (2004).
18. A. Jesacher, S. Fürhapter, S. Bernet, M. Ritsch-Marte, "Diffractive optical tweezers in the Fresnel regime," Opt. Express **12**, 2243-2250 (2004). http://www.opticsexpress.org/abstract.cfm?URI=OPEX-12-10-2243.
19. L. Paterson, M. P. MacDonald, J. Arlt, W. Sibbett, P. E. Bryant, and K. Dholakia, "Controlled rotation of optically trapped microscopic particles," Science **292**, 912-914 (2001).
20. R. Newell, J. Sebby, and T. G. Walker, "Dense atom clouds in a holographic atom trap," Opt. Let. **28**, 14, 1266-1268 (2003).
21. M. P. MacDonald, G. C. Spalding, K. Dholakia, "Microfluidic sorting in an optical lattice," Nature **426**, 421-424 (2003).
22. P. T. Korda, M. B. Taylor, D. G. Grier, "Kinetically locked-in colloidal transport in an array of optical tweezers," Phys. Rev. Lett., **89,** 128301 (2002).
23. H. F. Talbot, Philos. Mag., **9**, 401-407 (1836).
24. K. Patorski, The self-imaging phenomenon and its applications, Progress In Optics **XXVII**, 1-108 (1989).
25. R. Piestun and J. Shamir, "Generalized propagation invariant wave-fields," JOSA A., **15**, 3039-3034 (1998).
26. M. V. Berry and S. Klein, "Integer, fractional and fractal Talbot effects," J. Mod. Opt., **43**, 10, 2139-2164 (1996).
27. J. Leach, M. Dennis, J. Courtial, and M. Padgett, "Vortex knots in light," New J. Phys. **7**, 55.1-55.11 (2005).

1. Introduction

Optical tweezers were first demonstrated by Ashkin nearly 20 years ago [1]. Most tweezers systems reported to date rely on the gradient force produced by a tightly focused laser beam, acting on a dielectric particle, to create a three-dimensional (3D) trap near the beam focus. Other successful implementations include trapping particles in the local maxima of interference patterns [2-4] or in Laguerre Gaussian beams [5-7]. To trap large numbers of particles, an ideal optical potential is a periodic array. Such patterns can be generated by the interference of multiple plane-waves. In this paper, we use a collection of eighteen collimated beams to create the interference pattern, which is periodic both laterally and axially, enabling 3D trapping of multiple particles. In addition, by including higher spatial harmonics we create higher intensity gradients as well as transversely and axially localized traps. Therefore, the large number of planes waves means that we can form optical traps that are both brighter and narrower than those which would result from a sinusoidal fringe pattern.

In recent years, there has been a resurgence of interest in optical trapping because computer addressable spatial light modulators (SLMs) make possible the creation of multiple traps that can be steered individually [8-11]. The addressability of these SLMs is in contrast to the earlier work using static diffractive optics [12] or axicons which could only produce fixed patterns of traps. The ability to introduce focal power with the SLM also means that the traps can be manipulated axially allowing controlled 3D positioning within the sample cell volume, typically over a range of several 10's microns [13]. Complicated 3D structures can be assembled in this way and manipulated [14]. In principle diffractive optical elements can modulate either the phase or intensity of the light to generate 3D fields [15], but for applications such as tweezers, where the overall optical efficiency is important, it is standard to use SLMs as phase modulators, typically diffracting over 40% of the incident light into the optical traps.

#6962 - $15.00 US Received 24 March 2005; revised 4 May 2005; accepted 5 May 2005

Most holographic optical tweezers set-ups place the trapping sample in the Fourier-plane of the SLM in such a way that a linear phase introduced at the SLM results in a lateral displacement of the optical trap. This Fourier-relationship means that calculation of the holographic pattern transferred to the SLM is computationally intensive; therefore arbitrary 3D distributions typically require a few milliseconds of calculation per trap.

Recently, there has been success in using both an image plane and a Fresnel plane geometry. If the SLM is placed in the image plane of the traps and used in phase modulation mode with a phase-contrast filter in the Fourier plane, a small π-phase spot written to the SLM can specify a trap, producing a bright spot in the trapping plane [16]. Clearly, this phase-contrast approach requires only limited computation. Axial positioning is more problematic, however, and relies on the radiation pressure of counter-propagating beams [17]. Moreover, this technique uses low numerical aperture optics with typically lower lateral resolution.

Successful optical tweezers systems have also been implemented by trapping particles in the Fresnel region of a SLM. Placing the sample plane slightly displaced from the Fourier plane of the SLM provides some of the advantages of both the Fourier plane approach and the phase contrast image approach [18]. In our experimental set-up we also place the sample in a Fresnel region, but instead of a small detuning from the Fourier plane, we use a small detuning from the image plane. Moreover, this setup is also suitable for array trapping in three dimensions.

As an alternative to using a tightly focused laser beam to form a single localized trap, tweezers have also been implemented based on interference patterns formed between two or more beams [2-4]. This strategy has been applied to form large arrays of two-dimensional traps, but to our knowledge has not been extended to full 3D trapping. Controlling the relative phase of the beams allows the interference patterns to be translated, or in the case of helically phased beams, rotated [19]. The interferometric approach becomes more interesting for the creation of large arrays, where the aperture of the focusing lens does not fundamentally limit the field of view of the trapping field. Another advantage of interference fields over focused beams is that the intensity modulation in the axial direction can be total, which might be critical for the trapping of smaller particles (<500 nm) or atoms [20]. Most recently, multiple optical beams have been generated and combined using discrete optical components to create extended optical lattices for particle sorting [21], which may have an advantage over earlier sorting schemes using the Fourier configuration [22].

2. Optical trap design

To analyze optical lattices, we look at their plane wave components in k-space and then Fourier transform to obtain the optical fields in real space. Within k-space, every monochromatic plane wave component lies on the surface of a sphere and can be described by a radial and axial wave vector, such that,

$$k_0 = \sqrt{k_r^2 + k_z^2} \tag{1}$$

where k_r is the radial and k_z is the axial wave vector.

For beams falling within the paraxial limit the value of k_z is hence given by

$$k_z \cong k_0 - k_r^2 / 2k_0 \tag{2}$$

For a trapped array of objects, the desired optical field is a 3D distribution of local intensity maxima throughout the sample volume. We chose to create a hexagonal lattice,

#6962 - $15.00 US Received 24 March 2005; revised 4 May 2005; accepted 5 May 2005

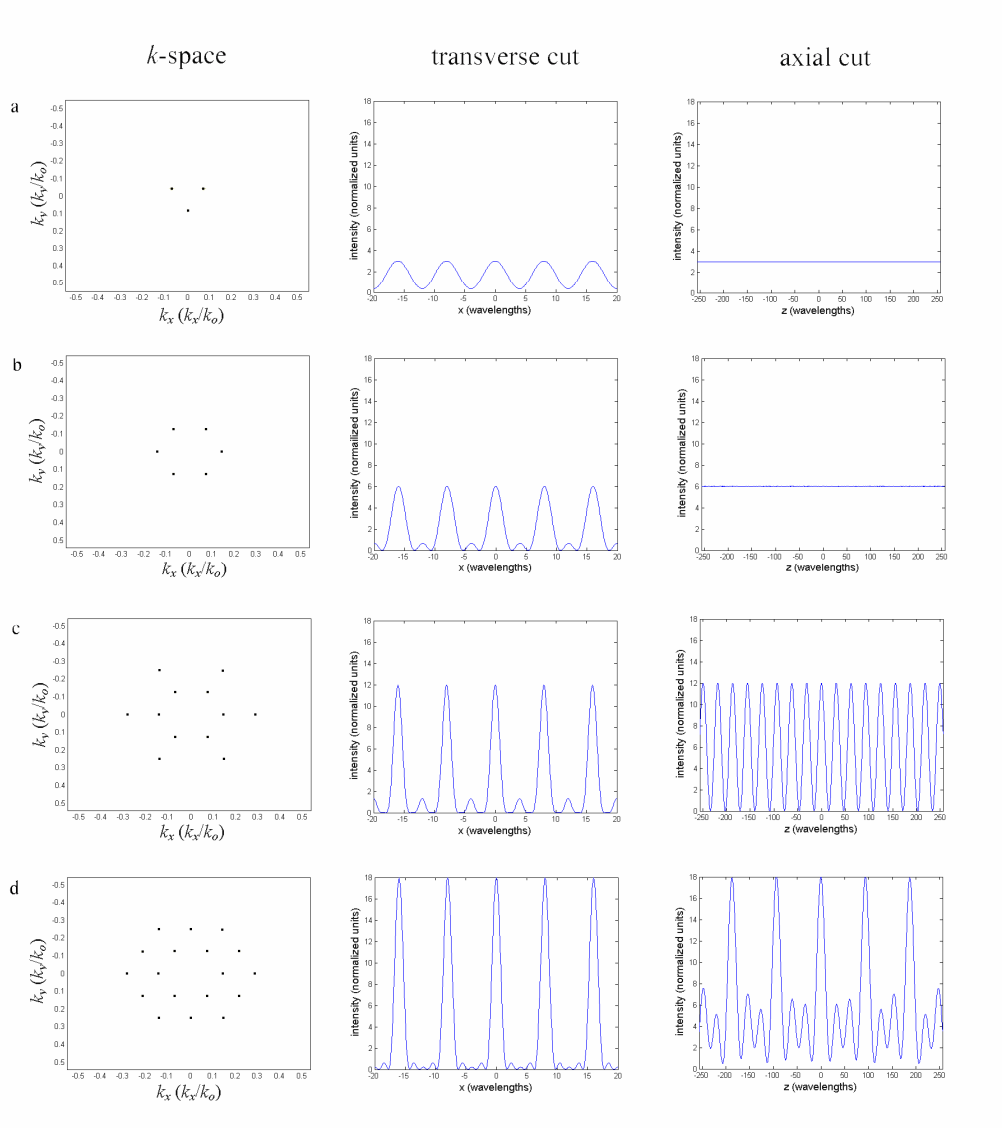

Fig. 1. Illustration of four different plane wave configurations that form hexagonal lattice structures. Each configuration is described by its *k*-space representation (left column), by a transverse cut (center column) and an axial cut (right column) of the intensity distribution each taken through a lattice vector direction. (a) The simplest configuration of three waves in *k*-space, which results in a sinusoidal transverse intensity pattern and a uniform axial profile. (b) A 6-wave configuration giving sharper peaks with small sidelobes transversely and similarly a uniform axial profile. (c) A 12-wave configuration formed by adding the second k-space harmonic of the fundamental hexagon, which increases the peak intensity of the traps but the does not eliminate the sidelobes. Having a second value of k_z results in a sinusoidal modulation in the axial intensity. (d) Our experimental configuration with 18 waves containing three values of k_z, giving the sharpest peaks and virtually eliminating the transverse sidelobes. The three values of k_z, make the Talbot image revival more complicated and give a larger axial periodicity. All intensity plots have been scaled so that there is equal power in each configuration. The transverse periodicity in (a), (b), (c), and (d) is 8λ; the axial periodicity in (c) is 32λ, while the axial periodicity in (d) is 94λ.

#6962 - $15.00 US
Received 24 March 2005; revised 4 May 2005; accepted 5 May 2005

which in its most simple form requires three interfering waves whose spatial frequency components lie on the vertices of an equilateral triangle. The resulting interference pattern has a sinusoidal modulation of its intensity along the lattice vector directions. Incorporating additional beams can make these maxima better defined but more importantly, can introduce an axial intensity modulation such that these maxima become localized in 3D, forming a 3D rather than a 2D trapping potential.

Figure 1 details the transverse and axial intensity sections of the interference pattern for four different plane-wave configurations, all of which produce hexagonal lattices. In all cases the sections were chosen so that they passed through the points of peak intensity. The intensity distributions in Fig. 1 are calculated using infinite extent plane waves, which give an approximation to the optical field in the regions close to the optical axis and the image plane, and were shown to be consistent with the experimental results. Two-dimensional arrays of particles have been formed in configurations similar to that shown in Fig 1(a) [2], but this geometry gives no axial intensity modulation, therefore 3D trapping is not possible. By including additional waves in the interference pattern, the sharpness and peak values of each maximum are increased, as shown in Fig. 1. The axial interference pattern can also be modulated to form a sinusoidal pattern [Fig. 1(c)], or a sharp-peaked quasi-periodic pattern [Fig. 1(d)]. For the experiment described in this paper, we used the configuration of Fig. 1(d) because it has the sharpest maxima both transversely (with minimal sidelobes) and axially. The six beams of the inner hexagon have the same magnitude of radial wavevector, $k_r(1)$. The six outer beams at the corners of the outer hexagon have radial wavevectors $k_r(3) = 2k_r(1)$, whilst the six beams at the mid points of the outer hexagon have radial wavevectors $k_r(2) = \sqrt{3}k_r(1)$.

Our hexagonal array of traps is effectively an image with lateral periodicity. Such images are known to reform in the near-field, at periodic distances of propagation; known as the Talbot effect [23-26]. This effect is best known in relation to periodic gratings where, in the near-field, the image of the grating in the x-y plane is repeated at periodic intervals of z. As a special implementation of the Talbot effect, our interference pattern exhibits similar behavior.

The Talbot effect applies to any image, or light distribution, where a decomposition in terms of plane waves gives values of k_z such that Δk_z between the various beams are rational fractions of each other [26]. This being the case, the image in any one plane is repeated in subsequent planes for which all the plane wave components are in phase again. In our eighteen-wave configuration we have three values of k_r with the ratio of $1:\sqrt{3}:2$ giving, from equation 2, two values of Δk_z, with respect to $k_r(1)$, in the ratio of 2:3. Over the Talbot distance, this means that the relative phase change between $k_r(1)$ and $k_r(2)$ is 4π and between $k_r(1)$ and $k_r(3)$ is 6π. The Talbot distance, z_{Talbot}, is hence given by

$$z_{Talbot} = \frac{2\pi}{\Delta k_z(1,3) - \Delta k_z(1,2)} \tag{3}$$

Most relevant to our application is that there is not a need to start with all the beams in phase. If the relative phase of the beams is set appropriately, i.e. in a ratio of 2:3, then at a particular propagation distance, and periodically with z_{Talbot} thereafter, the beams will be in–phase and constructively interfere to give the hexagonal lattice. Figure 2 shows the optical trapping fields obtained experimentally, which over the extent of a Talbot distance centered on the image plane, show good agreement with the plane wave model.

#6962 - $15.00 US Received 24 March 2005; revised 4 May 2005; accepted 5 May 2005

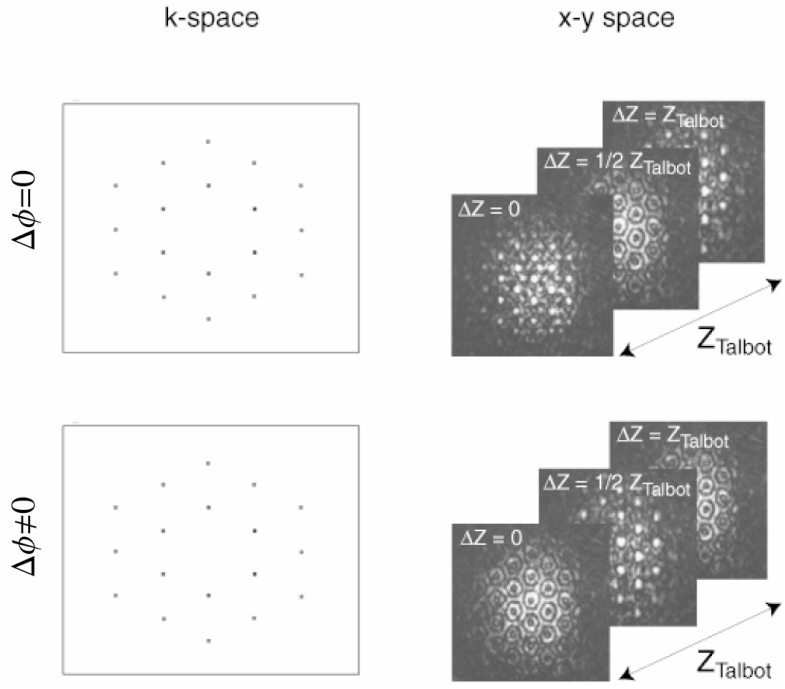

Fig. 2. The interference patterns produced when (a) all three sets of beams are in phase ($\Delta\Phi=0$) and the image at the half Talbot distance is the phase contrast image, and (b) when the phase is set to give the half Talbot image. In the later instance, the hexagonal trapping pattern is recovered after propagation through a fraction of the Talbot distance.

3. Hologram design

In this work we use a single SLM to create multiple, angularly displaced, plane-waves whose relative intensity and phase can be adjusted arbitrarily. By positioning the SLM near the image-plane of the traps, the beams interfere in the trapping plane to create the optical lattice. Even though implemented on a phase-only SLM, the algorithm we apply to calculate the hologram gives both intensity and phase control of the diffracted beams. It also produces high mode purity and reduced intensity in unwanted diffraction-orders. By deliberately programming the SLM to create the phase-contrast Talbot image of the array and defocusing the sample plane by a fractional-Talbot distance to recover the hexagonal lattice, we find that we can significantly increase the optical power in the trapping plane.

In all but a few special cases, when a phase-only SLM is programmed to produce a number of optical beams, the additional beams located at intermediate and related positions corrupt the desired pattern of optical traps in the Fourier-plane. When used to create multiple-beam interference patterns, these additional beams result in reduced contrast and significantly degrade the quality of the Talbot image revival. Recently, an algorithm that gives control over both the phase and intensity of the diffracted beams even when using a phase-only SLM has been reported [27]. After designing the diffractive optic (hologram) so that the first-order diffracted beam has the desired phase structure, the intensity at any point can be attenuated by adjusting the efficiency of the blazing in the corresponding region of the hologram.

Taking the plane of the SLM as the plane of interest, the initial stage in hologram design is to specify the desired weights, directions, and relative phases of the interfering beams, and calculate the phase distribution of the desired superposition, $\Phi(x,y)_{superposition}$. This phase distribution is then added to the phase distribution of a blazed diffraction grating $\Phi(x,\Lambda)_{grating}$, of period Λ. The first-order diffracted beam is then angularly separated from

#6962 - $15.00 US Received 24 March 2005; revised 4 May 2005; accepted 5 May 2005

the other orders, which are subsequently blocked using a spatial filter. The intensity distribution of the desired superposition is also calculated, $I(x,y)_{superposition}$, and normalized so the maximum intensity is unity. This intensity distribution, $I(x,y)_{superposition}$, is applied as a multiplicative mask to the phase distribution of the hologram, acting as a selective beam attenuator imposing the necessary intensity distribution on the first order diffracted energy. Thus the phase pattern applied to the SLM to create the desired hologram is approximated by [27].

$$\Phi(x,y)_{holo} = \pi + \left(\left(\Phi(x,y) + \Phi(x,\Lambda)\right)_{\mathrm{mod}\,2\pi} - \pi\right) \times \mathrm{sinc}^2\left(\left(1 - I(x,y)\right)\pi\right) \tag{4}$$

Unfortunately, the overall effect of the mask multiplication (sinc^2 term in Eq. 4) is that optical energy is diverted into the zero order and removed by a spatial filter, significantly reducing the optical efficiency of the hologram. The addition of further beams into the superposition usually increases the range of intensity within the interference pattern, such that the subsequent normalization and attenuation process further reduce the efficiency. In applications such as optical tweezers where the overall optical efficiency limits the number of traps that can be created using a laser of fixed power, diffraction efficiency is critical.

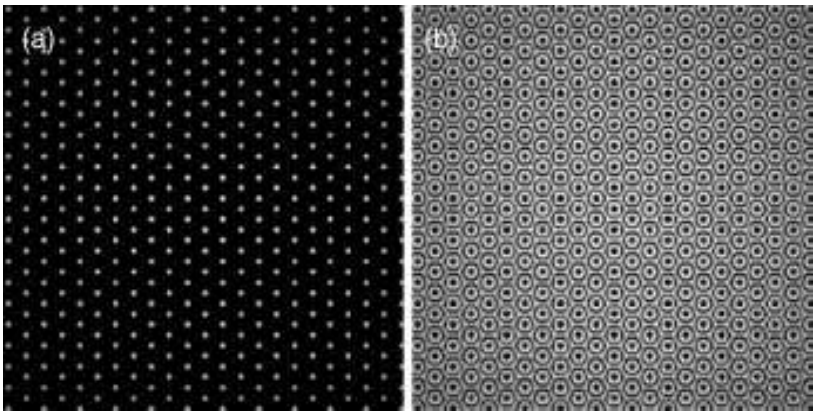

Fig. 3. (a) Intensity distribution of the interfering beams in the image plane of the SLM where all the 18 beams are in phase. (b) A similar distribution when the phase of all 18 beams are set to be midway between Talbot images. It is this image (b), with the addition of a linear phase, that forms the multiplicative mask upon which the hologram design is derived.

In our application we can vary the relative phase of three sets of beams, such that the total energy diffracted into the first order is maximized. This maximization occurs for the relative phasing which results in the intensity distribution being evenly distributed across the field (i.e. not the hexagonal lattice of traps). This typically occurs when the relative phase is set to give an inverse image. Irrespective of the relative phase of the hexagons, as discussed above, the hexagonal lattice is reformed in a near-by plane. The eighteen-plane wave geometry discussed above has a near uniform dark background, which when inverted produces a near uniform bright background resulting in an improved diffraction efficiency (see Fig. 3). However, despite taking advantage of this additional degree of freedom, the resulting optical efficiency of the arrangement is approximately half of that which can be achieved by placing the SLM in the Fourier-plane. The advantage of this algorithm over those based on Fourier-plane SLM's is that it is non-iterative, i.e. each pixel value is derived directly from equation (4) without need for repeated Fourier-transformation or other sophisticated search techniques. Irrespective of the number of traps produced, the calculation time for such a hologram at a resolution of 512x512 is only a few milliseconds.

#6962 - $15.00 US Received 24 March 2005; revised 4 May 2005; accepted 5 May 2005

4. Experimental configuration

The optical trapping setup was built around a 1.3NA, x100, Zeiss Plan Neofluar oil immersion microscope objective in an inverted configuration as shown in Fig. 4. The sample cell was mounted on a piezoelectric stage that allowed 100 μm of travel in the *x, y* and *z*. Control of the piezoelectric stage means that once trapped, the array of particles can be moved both laterally and axially with respect to the background. The trapping laser was a frequency doubled Nd:YAG with a maximum output power of 1.5W at 532 nm. The laser output was expanded to slightly overfill the active area of the Holoeye LC-R 2500 SLM. A spatial filter, positioned at an intermediate telescope, removed any unwanted diffraction orders. Taking into account the diffraction efficiency of the SLM, the use of a phase hologram algorithm, and the losses in the optical system, the laser power in the trapping plane was of the order of 150 mW, distributed among all the traps. The diffraction efficiency of the SLM with the designed hologram was about 40%. The NA of the outer beams was approximately 0.25, giving a hexagonal lattice with a period along the direct lattice vector of approximately 4 microns. Setting the phase difference between $k_r(1)$ and $k_r(2)$ at 2.1 radians and between $k_r(1)$ and $k_r(3)$ at 3.2 radians means that the trapping plane needs to be defocused by approximately 7μm to recover the hexagonal trapping lattice.

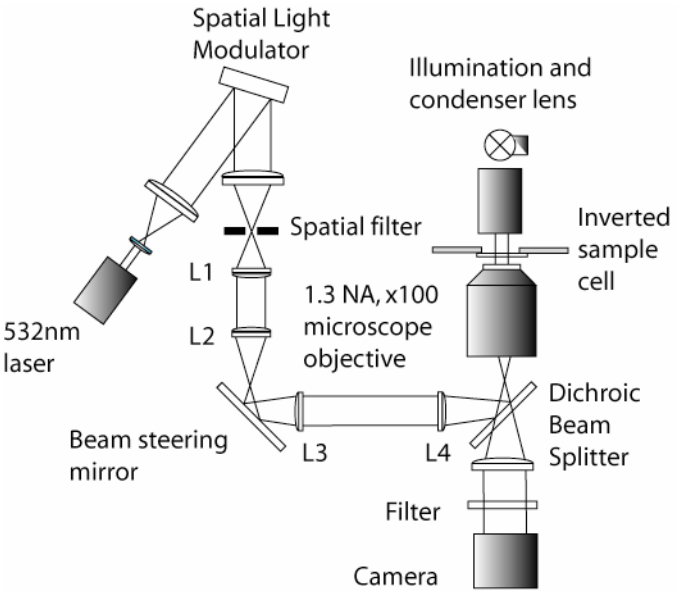

Figure 4: Schematic of the optical tweezers 4f setup. The lens L1, L2, L3 and L4 have focal lengths of 100mm, 160mm 140mm and 80mm respectively.

5. Results

We used the sharply peaked interference fields described in Sec. 2 to trap collections of micron-sized particles in planar triangular lattice configurations and later used them to translate the array patterns in 3D. Figure 5 shows three different patterns trapped in the hexagonal array. The trapping lattice has approximately 25 trap locations where all 18 of the plane waves overlap in the field of view of the microscope objective. Because the experimental set-up gives access to the image plane at an intermediate distance, we can selectively load the beads into the lattice by exposing only the necessary traps.

#6962 - $15.00 US Received 24 March 2005; revised 4 May 2005; accepted 5 May 2005

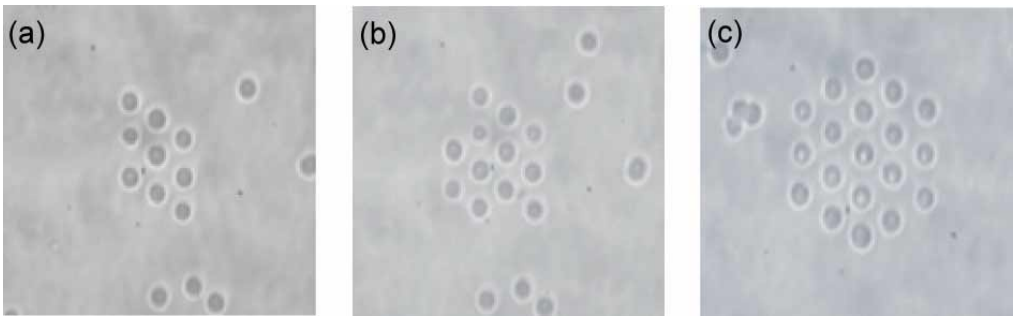

Fig. 5. Multiple patterns of 2 μm diameter silica spheres trapped in the hexagonal interference pattern. (a) A 9-sphere array, (b) A 12-sphere arrow pattern array, and (c) a 19-sphere hexagonal array.

Once the beads have been loaded, the crystalline structure is relatively robust owing to the 3D intensity gradient of each trap. Figure 6 shows the transportation of an array of 15 trapped beads where the sample cell is translated in all three Cartesian directions and the crystalline structure stays at the center of the field of view. Because of the axial intensity gradient, the structure can be lifted up and over other non-trapped beads.

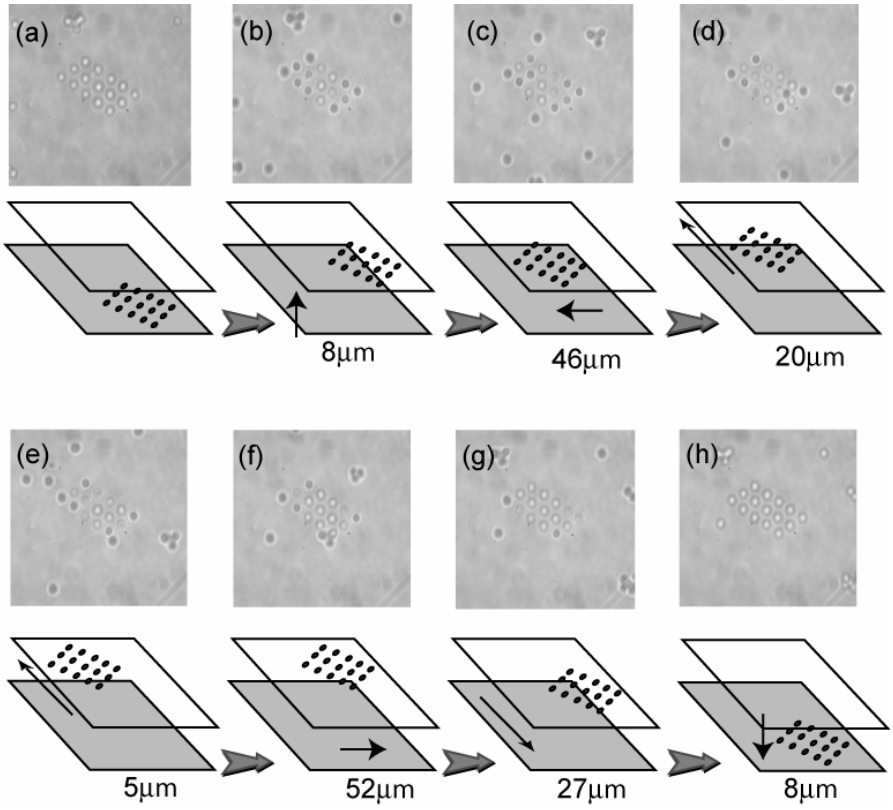

Fig. 6. A square array structure consisting of 15 2 μm diameter silica spheres trapped in a hexagonal interference pattern. (a) The structure is lifted axially by 8μm. (b) Structure is moved to the left by 46 μm. (c) Structure then moved in the positive y direction by a total of 25μm, (d)-(e). Array was then moved right by a total of 52 μm. (f) Structure then moved in the negative y direction by 27 μm,(g), before being lowered by 8 μm back down to its original position (h).

#6962 - $15.00 US Received 24 March 2005; revised 4 May 2005; accepted 5 May 2005

6. Conclusions

By combining multiple plane-waves, and utilizing the phase contrast Talbot image, we have demonstrated that it is possible to obtain 3D trapping of particles in interferometric optical tweezers without the need for counter propagating beams. By appropriately choosing the hologram algorithm, many interfering beams can be produced using a single SLM without unduly compromising the overall optical efficiency.

Within our optical tweezers application, the obscuration of the beams by the trapped micron-sized objects means that the Talbot effect in subsequent planes is destroyed and multiple planes of objects cannot be trapped in this way. However, for objects that perturb the transmitted light by only a small amount, e.g. atoms, this is not the case. The same experimental setup of a single SLM could be applied to generate a 3D lattice where the individual planes are simply separated by the Talbot image revival distance.

Compared to conventional optical tweezers, where the traps are formed in the Fourier-plane of the SLM, this approach may offer an advantage in the creation of large periodic array structures.

#6962 - $15.00 US Received 24 March 2005; revised 4 May 2005; accepted 5 May 2005